Star Formation through Time
*ASP Conference Series, Vol. **VOLUME**, 2003*
Pérez, González Delgado, Tenorio-Tagle

arXiv:astro-ph/0303322v1 14 Mar 2003

High Resolution Simulations of the Global and Local ISM

Miguel A. de Avillez

Department of Mathematics, University of Évora, R. Romão Ramalho 59, 7000 Évora, Portugal

Dieter Breitschwerdt

Max-Planck-Institut für Extraterrestrische Physik, Postfach 1312, D-85741 Garching bei München, Germany

Abstract. We present the first to date high resolution calculations of the ISM down to scales of 0.625 pc of the global and local ISM. The simulations show the morphology and structure of the different ISM phases and reproduce many of the features that have been observed in the Milky Way and other galaxies. In particular, they show that the hot gas has a moderately low volume filling factor ($\sim 20\%$) even in the absence of magnetic fields. Also, cold gas is mainly concentrated in filamentary structures running perpendicular to the midplane forming and dissipating within $\sim 10-12$ Myr. Compression is the dominant process for their formation, but thermal instability also plays a rôle. Also the evolution of the Local Bubble is simulated by multi-supernova explosions; calculated extensions after ~ 13 Myr match observations.

1. Introduction

Modelling the evolution of the ISM has a lot in common with meteorological studies. Both the troposphere and the interstellar gas exhibit time-dependent structures on all scales. In addition, both systems are heavily non-linear and subject to numerous instabilities in certain parameter regimes, which may lead to chaotic behaviour, while in others the evolution is fairly predictable. The key to a realistic description is in both cases highest possible spatial resolution and realistic input. The latter entails both the incorporation of all relevant physical processes and boundary conditions. This requires however the appropriate tools, which are computer clusters with parallelized hydrocodes and a sophisticated method of tracking non-linear structures, such as shock waves on the smallest possible scales. For more than 30 years there was the hope to reproduce the main features of the ISM by an analytical model, using simple recipes for the physical processes at hand, such as heating, cooling, conduction etc., along with simple solutions for the expansion of supernova remnants (SNRs), stellar winds and HII regions. In their seminal paper of a three-phase model regulated by supernova explosions in an inhomogeneous medium, McKee & Ostriker (1977, hereafter MO77) predicted a volume filling factor of the hot intercloud medium (HIM) of $f^V_{\rm HIM} = 0.7-0.8$. However, observations point to a value of ~ 0.5 (e.g.

Dettmar, 1992) or even lower when taking external galaxies into account. A way out has been suggested by Norman & Ikeuchi (1989) with the so-called chimney model, in which hot gas can escape into the halo. Indeed X-ray observations of several nearby edge-on galaxies have revealed extended, galaxy-sized halos (e.g. Wang et al. 2001). However, the transport of gas into the halo is still controversial, and arguments, that superbubble break-out may be inhibited by a large-scale disk parallel field have been put forward (e.g., Mineshige et al. 1993). On the other hand, it seems suggestive that although *initial* break-out may be difficult, any existing channel could be used by successive generations of SNe (see Breitschwerdt & Schmutzler 1999), venting material into the halo. Thus we believe that our simulations – without magnetic field – are indeed representative. We further stress the importance of a model box size of at least 1 kpc in and 10 kpc perpendicular to the plane. Thus we can be reasonably confident to capture both the largest structures (e.g., superbubbles and filaments) together with the smaller ones down to 0.625 pc. On a smaller scale, we show that simulating the Local Bubble in a *realistic* SN disturbed background medium makes a substantial difference to the case of a uniform ambient medium.

2. Numerical Simulations of a Supernova-Driven ISM

Code. This is a 3D HD code using adaptive mesh refinement (AMR) in a block-based structure in combination with Message Passing Interface (MPI) developed by Avillez (2003). The AMR scheme relies on virtual topologies of CPUs created through MPI (Message Passage Interface) calls. This approach uses two grid topologies: one defined by the $N_x \times N_y \times N_z$ blocks in which the computational domain is divided (each block is composed of $n_x \times n_y \times n_z$ cells) and the other composed of $N_x \times N_y \times N_z$ CPUs, each located at the centre of every block. When a refinement is required, a block is split into 8 (in 3D), 4 (in 2D) or 2 (in 1D) new blocks (children). This corresponds to an increase in linear resolution by a factor of two in the new blocks. Each child is associated to a new CPU. This process repeats itself until the finest level of resolution is reached. All the information relative to the tree structure is preserved in the virtual topology, being only necessary to query the different CPUs to learn their location in this topology, and therefore, the location of their neighbours, children and parents. At every new grid the procedure outlined above is carried out, followed by the correction of fluxes between the refined and coarse grid blocks. The adaptive mesh refinement scheme is based on Berger & Colella (1989) and in Bell et al. (1994). The gas dynamics part of the code uses the piecewise-parabolic method of Colella & Woodward (1984), a third-order scheme based on a Godunov method implemented in a dimensionally-split manner (Strange 1968) that relies on solutions of the Riemann problem in each zone rather than on artificial viscosity to follow shocks.

Model. The simulations described in this paper made use of the SN-driven ISM model of Avillez (2000), coupled to the three-dimensional block structured adaptive mesh refinement HD code for gas dynamics. The model includes a fixed gravitational field provided by the stars in the disk, radiative cooling (using Dalgarno & McCray 1972, with an ionization fraction of 0.1 for $T < 10^4$ K and a

cut-off at 10 K) assuming optically thin gas in collisional ionization equilibrium (CIE), and uniform heating due to starlight. Background heating due to starlight varies with z and is kept constant parallel to the plane, chosen such as to initially balance radiative cooling at 8000 K. The presence of background heating leads to the creation of thermally stable phases in the ISM, and therefore, the presence of a stable phase at low temperatures, leads to an increase in the amount of cold gas seen in these simulations in comparison to previous simulations (Avillez 2000). The gas is initially distributed in a smooth disk, taking into account the vertical distribution of the molecular, atomic (cool and warm), ionized and hot components of the ISM, as summarized in Dickey & Lockman (1990), Reynolds (1987) and Ferrière (1998). SNe Ia, Ib+c, and II are included with their observed distributions. The vertical distribution of SNe Ib+c and II depends on whether they are found in OB associations or isolated. 40% of them are placed at random locations distributed in an exponential distribution with a scale height of 90 pc. Clustered supernovae are set up in locations where the current local density is greater than 10 cm^{-3} with material still accreting ($\nabla \cdot \mathbf{v} < 0$) and a scale height of 46 pc. The number of stars in the association is determined from the overall mass inside a radius of the finest cell resolution, and using the Salpeter IMF the time interval between successive explosions is obtained. No density threshold is used to determine the location where isolated SNe should occur, because their progenitors drift away from the parental association. Similarly, later SNe in associations are no longer determined by gas density. The rates of SNe are taken from Capellaro et al. (1997) and are normalized to the volumes of the stellar disks of the different SNe populations used in the simulations. Individual SNRs are set up at the beginning of their Sedov phases, with radii determined by their progenitor masses, which are injected into the location of the explosion.

3. Simulations

Two runs are presented here: a 0.625 pc resolution simulation of the ISM and a Local Bubble (LB) simulation where an IMF appropriate for the Subgroup B1 of Pleiades (thought to be responsible for the formation of the Local Bubble cavity (Berghöfer & Breitschwerdt 2002) is used.

3.1. Local Bubble (LB) Simulations

Modelling. A total of 20 stars with masses between 10 and 20 $M_{\odot}$ explode at $x = 220$, $y = 400$ pc (see Fig. 1) thus generating the Local Cavity into which the LB will expand. The Galactic SN rate has been used for the setup of *other SNe* in the remaining of the disk. These runs (over 25 Myrs) made use of the 3D parallel AMR scheme described above with the finest resolution being 1.25 pc. The grid has $0 \leq x,\ y \leq 1$ kpc, $|z| \leq 10$ kpc and periodic boundary conditions along the vertical direction and free conditions at z_{min} and z_{max}.

Results. The locally enhanced SN rate produces a coherent LB structure within a highly disturbed background medium (due to ongoing star formation). Successive explosions heat and pressurize the LB, which at first looks smooth, but develops internal structure at $t > 8$ Myr. After 13.5 Myr 20 SNe have occurred inside the LB, filling a volume roughly corresponding to the present day

Figure 1. *Left:* 10^5 yrs after the first star, with $M = 20\,M_\odot$, exploded at $x = 240$, $y = 400$ pc, defining the origin of the LB. *Right:* The LB at $t = 13.50$ Myr after the 20th supernova of a 10 $M_\odot$ progenitor star, occurred.

LB (Fig. 1). The LB is still bounded by a shell which starts to fragment due to Rayleigh-Taylor instabilities after the last explosion. Clouds and cloudlets of various sizes are formed when dense shells of bubbles collide, as has been predicted by Breitschwerdt et al. (2000).

3.2. Global ISM Simulations at 0.625 pc Resolution

Modelling. The simulation grid has an area of 1 kpc^2, centered on the Sun, with a vertical extension between ±10kpc. Boundary conditions are periodic perpendicular to the midplane and free conditions at the bottom and top boundaries. Four runs with SN rates of 1, 2, 4, 8, and 16 times the Galactic rate were carried out using four levels of refinement yielding a resolution of the finest AMR level of 0.625 pc. The simulation time was 400 Myr.

Results. The simulations reproduce many of the features that have been observed in the Galaxy and other galaxies, namely: (i) A thick frothy gas disk composed of a warm, neutral medium overlying a thin HI disk, with a variable thickness up to $\sim$ 80 pc; (ii) bubbles and superbubbles and their shells distributed on either side of the midplane; (iii) tunnel-like structures (chimneys) crossing the thick gas disk and connecting superbubbles to the upper parts of the thick gas disk; (iv) thick gas disk with a distribution compatible with the presence of two phases having different scale heights: a neutral layer with $z_n \sim 500$ pc (warm HI disk) and an ionized component extending to a height $z_i \sim 1.5$ kpc above the thin HI disk; (v) cold gas mainly concentrated into filamentary structures running perpendicular to the midplane (Fig. 2 - the figure shows density and temperature maps of midplane taken at 117 Myr of evolution). These clouds form and dissipate within some 10-12 Myr. Compression is the dominant process for their formation, but thermal instability also plays a rôle; (vi) most

Figure 2. Density (left) and temperature (right) maps of the Galactic plane for $\sigma/\sigma_{Gal} = 2$ at $t = 117$ Myr. The finest resolution is 0.625 pc.

remarkably, the hot gas has moderately low volume filling factor in agreement with observations ($\sim 20\%$) even in the absence of magnetic fields (left panel of Fig. 3) and is mainly distributed in an interconnected tunnel network and in some case it is confined to isolated bubbles (Fig. 2). With the increase of the supernova rate to four times the galactic rate the volume of occupation of the hot gas increase to some 30%, which is still way below the predictions of MO77.

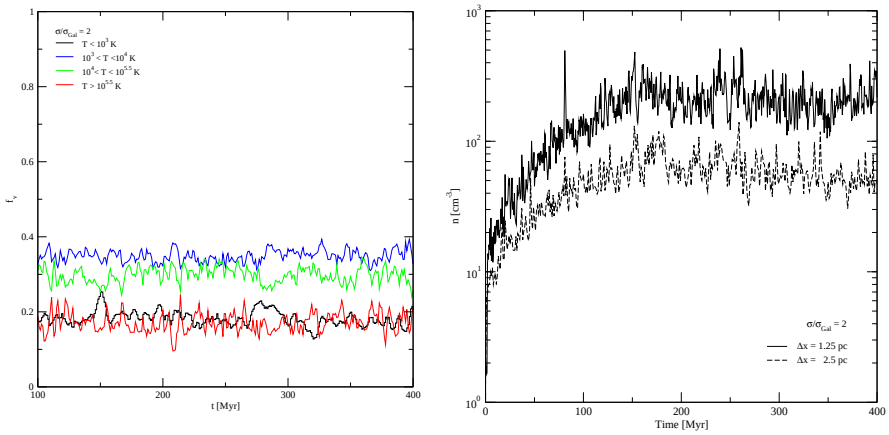

Figure 3. *Left:* Time evolution of the volume filling factors of T$\leq 10^3$ K, 10^3 <T$\leq 10^4$ K, 10^4 <T$\leq 10^{5.5}$ K, T> $10^{5.5}$ K gases for $\sigma/\sigma_{Gal} = 2$. *Right:* Comparison between maximum density (for $\sigma/\sigma_{Gal} = 2$) for two intermediate grid resolutions 1.25 pc (solid) and 2.5 pc (dashed).

The simulations also show how crucial spatial resolution is in order to capture small scale structures and, in particular, the cold gas. A comparison be-

tween the maximum density measured at two intermediate levels of refinement: 1.25 pc and 2.5 pc show that an increase in resolution by a factor of two implies an increase in the maximum density and a decrease in minimum temperature of the gas by factors greater than 5 (right panel of Fig. 3).

4. Final Remarks

The model developed thus far did not take into account the Galactic differential rotation nor the effects of magnetic fields and non-equilibrium ionization cooling. The latter is particularly important because radiative cooling is based on CIE. Therefore gas dynamical changes on time scales less than the atomic scales (e.g., for ionization, recombination, etc.) will drive the plasma out of equilibrium and yield incorrect cooling rates. Thus a self-consistent dynamical and thermal description of the plasma is necessary (see Breitschwerdt & Schmutzler 1999).

References

Avillez, M.A., 2000, MNRAS, 315, 479

Avillez, M.A., 2003, J. Comp. Phys., in prep.

Berger, M.J., & Colella, P., 1989, J. Comp. Phys. 82, 64

Bell, J., Berger, M., Saltzman, J., & Welcome, M., 1994, SIAM J. Sci. Comp., 15, 127

Berghöfer, T., & Breitschwerdt, D., 2002, A&A 390, 299

Breitschwerdt, D., Schmutzler, T., 1999, A&A 347, 650

Breitschwerdt, D., Freyberg, M.J., Egger, R., 2000, A&A 361, 301

Cappellaro, E., Turatto, M., Tsvetkov, D. Yu., Bartunov, O.S., Pollas, C., Evans, R., & Hamuy, M., 1997, A&A, 322, 431

Colella, P., & Woodward, P., 1984, J. Comp. Phys., 54, 174

Dalgarno, A., & McCray, R.A., 1972, ARA&A, 10, 375

Dettmar, R.-J., 1992, Fund. of Cosm. Phys. 15, 143

Dickey, J.M., & Lockman, F.J., 1990, ARA&A, 28, 215

Ferrière, K., 1998, ApJ, 503, 700

McKee, C.F., Ostriker, J.P., 1977, ApJ 218, 148 (MO77)

Mineshige, S., Shibata, K., Shapiro, P. R., 1993, ApJ 409, 663

Norman, C.A., Ikeuchi, S., 1989, ApJ 345, 372

Reynolds, R.J., 1987, ApJ, 323, 118

Strange, W.G., 1968, SIAM J. Numer. Anal., 5, 506

Wang, Q.D., Immler, S., Walterbos, R., Lauroesch, J. T., Breitschwerdt, D., 2001, ApJ, 555, L99

This figure "mavillez_fig1a.jpg" is available in "jpg" format from:
http://arXiv.org/ps/astro-ph/0303322v1

This figure "mavillez_fig1b.jpg" is available in "jpg" format from:
http://arXiv.org/ps/astro-ph/0303322v1

This figure "mavillez_fig2a.jpg" is available in "jpg" format from:
http://arXiv.org/ps/astro-ph/0303322v1

This figure "mavillez_fig2b.jpg" is available in "jpg" format from:
http://arXiv.org/ps/astro-ph/0303322v1